CHEMISTRY
A EUROPEAN JOURNAL

DOI: 10.1002/chem.200902788

Cyclometalated Ir^{III} Complexes with Substituted 1,10-Phenanthrolines: A New Class of Efficient Cationic Organometallic Second-Order NLO Chromophores

Adriana Valore,[a] Elena Cariati,[a] Claudia Dragonetti,[a] Stefania Righetto,[a] Dominique Roberto,*[a] Renato Ugo,[a] Filippo De Angelis,*[b] Simona Fantacci,[b] Antonio Sgamellotti,[b] Alceo Macchioni,*[c] and Daniele Zuccaccia[c]

Dedicated to the Centenary of the Italian Chemical Society

Abstract: Cyclometalated cationic Ir^{III} complexes with substituted 1,10-phenanthrolines (1,10-phen), such as [Ir(ppy)$_2$(5-R-1,10-phen)]Y (ppy = cyclometalated 2-phenylpyridine; R = NO_2, H, Me, NMe_2; $Y^- = PF_6^-$, $C_{12}H_{25}SO_3^-$, I^-) and [Ir(ppy)$_2$(4-R,7-R-1,10-phen)]Y (R = Me, Ph) are characterized by a significant second-order optical non linearity (measured by the electrical field induced second harmonic generation (EFISH) technique). This nonlinearity is controlled by MLCT processes from the cyclometalated Ir^{III}, acting as a donor push system, to π* orbitals of the phenanthroline, acting as an acceptor pull system. Substitution of cyclometalated 2-phenylpyridine by the more π delocalized 2-phenylquinoline (pq) or benzo[*h*]quinoline (bzq) or by the sulfur-containing 4,5-diphenyl-2-methyl-thiazole (dpmf) does not significantly affect the μβ absolute value, which instead is affected by the nature of the R substituents on the phenanthroline, the higher value being associated with the electron-withdrawing NO_2 group. By using a combined experimental (the EFISH technique and ^{1}H and ^{19}F PGSE NMR spectroscopy) and theoretical (DFT, time-dependent-DFT (TDDFT), sum over states (SOS) approach) investigation, evidence is obtained that ion pairing, which is controlled by the nature of the counterion and by the concentration, may significantly affect the μβ values of these cationic NLO chromophores. In CH_2Cl_2, concentration-dependent high absolute values of μβ are obtained for [Ir(ppy)$_2$(5-NO_2-1,10-phen)]Y if Y is a weakly interacting anion, such as PF_6^-, whereas with a counterion, such as $C_{12}H_{25}SO_3^-$ or I^-, which form tight ion-pairs, the absolute value of μβ is lower and quite independent of the concentration. This μβ trend is partially due to the perturbation of the counterion on the LUMO π* levels of the phenanthroline. The correlation between the μβ value and dilution shows that the effect of concentration is a factor that must be taken into careful consideration.

Keywords: density functional calculations · EFISH (electrical-field-induced second-harmonic generation) · ion pairs · iridium · nonlinear optics

[a] Dr. A. Valore, Prof. Dr. E. Cariati, Dr. C. Dragonetti, Dr. S. Righetto, Prof. Dr. D. Roberto, Prof. Dr. R. Ugo
Dip. Chimica Inorganica
Metallorganica e Analitica "Lamberto Malatesta"
Università di Milano, UdR dell'INSTM di Milano
and ISTM-CNR
via Venezian 21, 20133, Milano (Italy)
Fax: (+39) 02-50314405
E-mail: dominique.roberto@unimi.it

[b] Dr. F. De Angelis, Dr. S. Fantacci, Prof. Dr. A. Sgamellotti
ISTM-CNR, c/o Dipartimento di Chimica
Università di Perugia
via Elce di Sotto 8, 06123, Perugia (Italy)
Fax: (+39) 075-585-5606
E-mail: filippo@thch.unipg.it

[c] Prof. Dr. A. Macchioni, Dr. D. Zuccaccia
Dipartimento di Chimica
Università di Perugia
via Elce di Sotto 8, 06123, Perugia (Italy)
Fax: (+39) 075-585-5598
E-mail: alceo@unipg.it

Introduction

In the last 15 years, organometallic and coordination complexes have emerged as new interesting molecular chromophores with second-order nonlinear optical (NLO) properties, as they may offer, when compared to traditional organic second-order NLO chromophores, additional electronic effects or properties acting on the NLO response. These properties and effects, such as charge-transfer transitions between the metal and the ligands (usually at low energy and of relatively high intensity), are tunable by virtue of the nature, oxidation state, and coordination sphere of the metal center.[1]

For instance, coordination of a metal to second-order push–pull NLO chromophores, such as stilbazoles, bipyridines, phenanthrolines, and terpyridines bearing an NR_2 donor group, produces a significant increase of their NLO response, owing to a red-shift of the intraligand charge-transfer transition (ILCT) induced by the metal acting as a Lewis acceptor. Conversely, if the NLO chromophores bear a strong electron-acceptor group, the NLO response is mainly controlled by metal-to-ligand charge-transfer transitions (MLCT).[1]

Recently, various cationic cyclometalated Ir^{III} complexes with a phenanthroline ligand[2] have been shown to have interesting photoemissive properties. Density functional theory (DFT) investigations have shown that the HOMO of this class of new luminescent Ir^{III} complexes[2] is mainly an antibonding combination of Ir (t_{2g}) orbitals and π orbitals of the cyclometalated ligand, whereas the LUMO is a π* antibonding orbital of the chelated phenanthroline. Therefore transitions between the HOMO and the LUMO have a significant charge-transfer character and, as a consequence, these Ir^{III} complexes can behave as second-order NLO chromophores, in which the cyclometalated ligands act as donors towards the acceptor π system of the phenanthroline ligand. Several preliminary investigations[3–6] have confirmed that cationic cyclometalated Ir^{III} complexes with a substituted phenanthroline, and with various cyclometalated ligands, show a significant second-order NLO response, as determined in CH_2Cl_2 (10^{-3} M) by the electrical field induced second harmonic generation (EFISH) technique.[7] Significantly, this response is reached without any cost in transparency.[8]

Herein we present a thorough investigation on these new second-order NLO chromophores based on cyclometalated Ir^{III} complexes, in which the role of the substituents on the 1,10-phenanthroline and of the nature of the cyclometalated moiety, will be discussed. For these ionic NLO chromophores, ion pairing in a solvent such as CH_2Cl_2 could be relevant, consequently, we also report an investigation of the effect of different counterions ($C_{12}H_{25}SO_3^-$, I^-, or PF_6^-) and of the concentration on their second-order NLO response, by the use of a combination of EFISH and ^1H and ^{19}F pulsed field gradient spin echo (PGSE) NMR[9] techniques. DFT/time-dependent-DFT (TDDFT) calculations have been performed on the selected systems to provide insight into the electronic properties of these systems and to rationalize some of the experimentally observed trends. Our results allow us to make some general conclusions about the origin of the second-order NLO properties, and provide evidence of the significance effect of ion pairing on the overall NLO response.

Results and Discussion

Complexes [Ir(ppy or pq or bzq or ttpy or dpmt)$_2$(5-R-1,10-phen)][PF_6] (where ppy, pq, bzq, ttpy and dpmt are cyclometalated 2-phenylpyridine,[3] 2-phenylquinoline,[5] benzo[*h*]quinoline,[6] 3′-(2-pyridil)-2,2′:5′,2″-terthiophene,[5] and 4,5-diphenyl-2-methyl-thiazole,[4] respectively; 1,10-phenanthroline = 1,10-phen; R = Me, NO_2, H, NMe_2; Scheme 1) and [Ir(ppy or bzq)$_2$(4-R,7-R-1,10-phen)]PF_6[3,6] (R = Me, Ph),

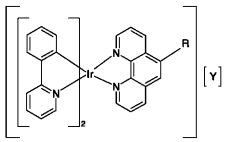

[Ir(ppy)$_2$(5-R-1,10-phen)]Y

1a R = Me **1b** R = NO_2
1c R = H **1d** R = NMe_2

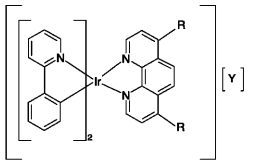

[Ir(ppy)$_2$(4-R,7-R-1,10-phen)]Y

1e R = Me **1f** R = Ph

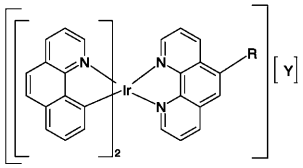

[Ir(bzq)$_2$(5-R-1,10-phen)]Y

2a R = Me **2b** R = NO_2

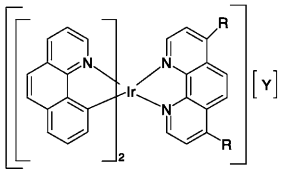

[Ir(bzq)$_2$(4-R,7-R-1,10-phen)]Y

2e R = Me **2f** R = Ph

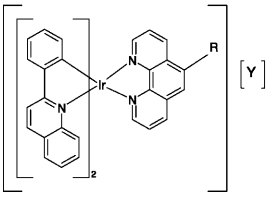

[Ir(pq)$_2$(5-R-1,10-phen)]Y

3a R = Me **3b** R = NO_2
3c R = H

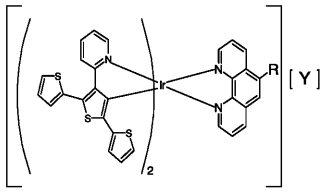

[Ir(ttpy)$_2$(5-R-1,10-phen)]Y

4a R = Me **4b** R = NO_2

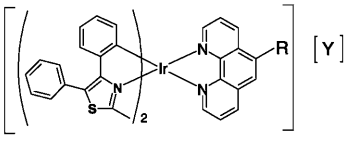

[Ir(dpmt)$_2$(5-R-1,10-phen)]Y

5a R = Me **5b** R = NO_2

Scheme 1. Cyclometalated Ir^{III} complexes investigated.

were prepared as previously described[3–6] by a two-step process: i) preparation of the chloro-bridged dimer [{Ir(cyclometalated ppy or bzq or pq or ttpy or dpmt)$_2$Cl}$_2$]; ii) bridge cleavage reaction with 5-R-1,10-phenanthroline or 4-R,7-R-1,10-phenanthroline. The complexes with other counterions ($C_{12}H_{25}SO_3^-$, I^-) were prepared in a similar manner, but using Na[$C_{12}H_{25}SO_3$] or KI instead of [NH_4][PF_6] (see the Experimental Section).The second-order NLO properties were determined by the EFISH technique[7] working with a non-resonant 1.907 μm wavelength in CH_2Cl_2 solution, a low polarity solvent, which allows the extension of the use of this technique to ionic compounds by virtue of the significant ion pairing.[1h] The EFISH technique can provide information on the intrinsic molecular NLO properties through Equation (1):

$$\gamma_{EFISH} = (\mu\beta_\lambda/5kT) + \gamma(-2\omega; \omega, \omega, 0) \quad (1)$$

in which $\mu\beta_\lambda/5kT$ is the dipolar orientational contribution and $\gamma(-2\omega; \omega, \omega, 0)$, a third-order term at a frequency ω of the incident wavelength λ (1.907 μm in this case), which is usually negligible for dipolar complexes, such as those investigated in this work. Thus, the product of the dipole moment (μ) times $\beta_{1.907}$, the projection of the vector component of the quadratic hyperpolarizability tensor along the dipole-moment vector, is the information given by the EFISH technique.

The relevant bands of the electronic absorption spectra along with the values of EFISH $\mu\beta_{1.907}$ for the various complexes investigated are reported in Table 1. All complexes display strong absorption bands between $\lambda = 250$ and 290 nm, attributed to π–π* ligand-centered (LC) transitions of the π systems of the 1,10-phenanthroline and of the cyclometalated ligands. Weaker absorption bands at longer wavelengths (in the range $\lambda = 300$–450 nm) have been attributed to metal-to-ligand charge-transfer transitions (MLCT), mainly from the Ir^{III} metal center to vacant π* orbitals of the phenanthroline ligand.[2] If the 1,10-phenanthroline carries a NR_2 donor group, an intraligand charge transfer (ILCT) from the NR_2 group to the π*-antibonding orbitals of the 1,10-phenanthroline also contributes to the absorption spectrum in the 350–450 nm region.[3]

As reported in our preliminary investigations,[3–6] all complexes show a negative second-order NLO response measured as $\mu\beta_{1.907}$ ($\mu\beta_{1.907}$ ranging from −1140 to -2230×10^{-30} D cm^5 esu^{-1}), but they do not show strong absorption bands above $\lambda = 450$ nm, so that a significant second harmonic generation may be obtained without any significant cost in transparency towards the strength of the second harmonic, a crucial aspect in the design of second-order NLO chromophores.[8]

It must be stressed that EFISH measurements of such ionic NLO chromophores do not allow the determination of the $\beta_{1.907}$ value, but only that of the product $\mu\beta_{1.907}$, since the concept, and therefore the experimental determination, of the dipole moment of ionic species is quite problematic, even in solvents of relatively low polarity such as CH_2Cl_2 or $CHCl_3$; although it is possible for certain ion-pairs of some compounds.[10] As our EFISH investigation only measures the projection of the vector component of the quadratic hyperpolarizability β tensor along the dipole moment vector, in some cases only partial information about the total second-order NLO properties can be found, since the relative orientation of the vector component of β with respect to the dipole vector axis plays a significant role (as an example, a reciprocal orthogonal orientation results in a zero EFISH response although β may have a significant magnitude). In the case of the Ir^{III} NLO chromophores investigated in this work there is no direct parallel between the vector component of β and the main dipole moment vector, as would occur in a classical 1D push–pull organic chromophore, therefore, the reciprocal orientation should always be taken into consideration when comparing absolute values of $\mu\beta_{1.907}$. With this in mind, for the series of structurally related

Table 1. Absorption spectra and EFISH $\mu\beta_{1.907}$ in CH_2Cl_2.

Ir^{III} complex	Y^-	Absorption maxima[a] [nm], [ε [M^{-1} cm^{-1}]]	EFISH $\mu\beta_{1.907}$[b] [10^{-30} D cm^5 esu^{-1}]
1a	PF_6^-	255 (sh), 268 [60300], 333 (sh), 377 [8070]	−1565
1a	$C_{12}H_{25}SO_3^-$	251(sh), 270 [39400], 333(sh), 376 [8270]	−1350
1b	PF_6^-	254 (sh), 264 [86900], 378 [12400]	−2230
1b	$C_{12}H_{25}SO_3^-$	253(sh), 261 [52700], 378 [7200]	−1430
1c	PF_6^-	252 (sh), 264 [58500], 377 [9130]	−1270
1d	PF_6^-	252 (sh), 264 [81400], 334 (sh)	−1330
1e	PF_6^-	255 (sh), 265 [73000], 375 (sh)	−1454
1f	PF_6^-	269 [51300], 282 (sh) 385 [9020]	−1997
2a	PF_6^-	256 [55000], 325 [17000], 417 [6600]	−1680
2a	$C_{12}H_{25}SO_3^-$	256 [67000], 321 [20900], 415 [7940]	−1219
2b	PF_6^-	256 [107000], 313 [34800], 408 [12900]	−1905
2b	$C_{12}H_{25}SO_3^-$	255 [69500], 310 [16000], 408 [7400]	−1389
2e	PF_6^-	255 [77700], 325 [22100], 417 [7250]	−1588
2e	$C_{12}H_{25}SO_3^-$	255 [70300], 321 [21700], 420 [8980]	−1140
2f	PF_6^-	259 [68300], 283 (sh), 333 [28200], 418 [8580]	−1720
2f	$C_{12}H_{25}SO_3^-$	259 [117000], 280 [80500], 325 [42200]	−1298
3a	PF_6^-	273 [70400], 329 [20700], 347(sh), 431 [4750]	−2090
3b	PF_6^-	268 [81100], 324 [27600], 430 [6930]	−1720
3c	PF_6^-	269 [95000], 330 [41300], 433 [14700]	−1850
4a	PF_6^-	260 [44500], 319(sh), 396 [17378]	−1320
4b	PF_6^-	257 [62300], 315 [28100], 397(sh)	−1640
5a	PF_6^-	261 [48000], 272(sh), 358 [9400]	−1414
5a	$C_{12}H_{25}SO_3^-$	265 [59400], 356 [12800]	−1220
5b	PF_6^-	262 [67200], 357 [15200]	−1780

[a] All complexes show a band tail above $\lambda = 400$ nm up to about $\lambda = 500$–550 nm. [b] By working at 10^{-3} M; the error of EFISH measurements is ±10%.

NLO chromophores, investigated in this work, only the general trends of the $\mu\beta_{1.907}$ values have been discussed.

The effect of the nature of the 1,10-phenanthroline substituents and of the cyclometalated ligands on the $\mu\beta_{1.907}$ values of cationic cyclometalated Ir^{III} chromophores with PF_6^- as counterion and the electronic origin of this effect: Here we briefly summarize and discuss the general trends of the $\mu\beta_{1.907}$ values of the various cationic cyclometalated Ir^{III} chromophores investigated up to now (Scheme 1) with PF_6^- as the counterion (Table 1). If the cyclometalated ligand is 2-phenylpyridine, a particularly high $\mu\beta_{1.907}$ absolute value is measured by the EFISH technique for complex **1b**-PF_6, with a 1,10-phenanthroline carrying a nitro group. The $\mu\beta_{1.907}$ absolute values of complexes with other 1,10-phenantrolines, such as $[Ir(ppy)_2(5\text{-Me-1,10-phen})][PF_6]$ (**1a**-PF_6) and $[Ir(ppy)_2(4\text{-Me,7-Me-1,10-phen})][PF_6]$ (**1e**-PF_6) are quite similar, suggesting that the effect of the number and position of methyl substituents is negligible, whereas an increase in the π delocalization on the 1,10-phenanthroline ligand leads to an increase of the absolute value of $\mu\beta_{1.907}$, as evidenced by comparing $[Ir(ppy)_2(4\text{-Ph,7-Ph-1,10-phen})][PF_6]$ (**1f**-PF_6) with (**1e**-PF_6) (Table 1).

Comparison of various structurally related cyclometalated ligands with the same 1,10-phenanthroline ligand (Table 1), but with π systems of different size, indicates that there is not a significant effect on either the sign or absolute value of $\mu\beta_{1.907}$. The $\mu\beta_{1.907}$ value only slightly increases if the ligands cyclometalated 2-phenylquinoline (**3a**-PF_6 and **3c**-PF_6) or cyclometalated benzo[*h*]quinoline (**2a**-PF_6) are considered rather than the cyclometalated 2-phenylpyridine (**1a**-PF_6 and **1c**-PF_6). When the cyclometalated ligands are not structurally related, as in the case of **4** and **5**, the absolute $\mu\beta_{1.907}$ value becomes lower (Table 1).[5]

Insight into the electronic origin of the above trends, has been obtained by DFT, TDDFT, and sum over states (SOS) calculations, performed on the **1a**–**1f**, **3a**–**3c**, **4a**–**4b**, and **5a**–**5c** cations.[11] The investigated Ir^{III} NLO cationic chromophores have a common electronic characteristic, they have a similar pattern of frontier molecular orbitals in relation to the phenanthroline substituents.[3–5] In particular, the HOMO of all the cations is composed of an antibonding combination of Ir (t_{2g}) orbitals and π orbitals of the cyclometalated ligand, whereas the LUMO and LUMO+1 are π^* antibonding orbitals of the 1,10-phenanthroline. In **1b** with a 1,10-phenanthroline carrying a NO_2 group, these two phenanthroline π^* LUMOs strongly mix with the NO_2 antibonding orbital, producing a stabilization of all the phenanthroline π^* orbitals, which leads to a reduction by more than 1 eV of the HOMO–LUMO gap compared to **1d** with the phenanthroline carrying a NMe_2 group. For **1b**, the EFISH quadratic hyperpolarizability is exclusively the sum of negative contributions,[3] resulting in an overall negative value, as found experimentally. The largest contributions arise from MLCT excitations involving the π^* phenanthroline orbitals, as acceptors, with a large increase of the excited state dipole moment compared to the ground state. The negative sign of the EFISH quadratic hyperpolarizability arises from the scalar product of the vector component β_{vec} and the ground state dipole moment, which have opposite directions. Indeed, while the ground state dipole moment goes from the Ir-cyclometalated system to the phenanthroline, upon MLCT excitation a negative charge accumulates on the phenanthroline, which leads to a reversal of the sign of the excited state dipole moment, controlling β_{vec}, when compared to the direction of the ground state dipole moment.[1a]

For **1d**, counteracting positive (ILCT) and negative (MLCT) contributions to the EFISH quadratic hyperpolarizability are calculated, with the latter controlling the negative sign of the converged final value, in agreement with the negative value of $\mu\beta_{1.907}$ found experimentally (Table 1). Such opposite contributions are the origin of the much smaller $\mu\beta_{1.907}$ absolute value of **1d** compared to that of **1b** (Table 1). Since **1b** and **1d** are structurally similar, although the dipole moment of **1b** and **1d** is likely significantly different.[3] Additionally, the value of $\beta_{1.907}$ must be significantly different for the two compounds, as inferred from the rather different absolute values of $\mu\beta_{1.907}$ (Table 1).

The decrease of the absolute $\mu\beta_{1.907}$ values observed (Table 1) on going from **1a** and **1b**, with a cyclometalated 2-phenylpyridine (ppy), to **4a** and **4b**, with a cyclometalated 3′-(2-pyridil)-2,2′:5′,2″-terthiophene (ttpy), can be attributed to the significant stabilization of the HOMO, which is still a combination of the Ir (t_{2g}) and cyclometalated ligand, but with a reduced metal character, owing to the extended π conjugation of ttpy.[5] The LUMO and LUMO+1, in contrast to the HOMO, are not affected too much by the nature of the cyclometalated ligand.

In conclusion, in these new cationic Ir^{III} second-order NLO chromophores, the substituted 1,10 phenanthroline and the cyclometalated ligands can be separately modified without any relevant mutual effect, thus allowing a predictable tuning of the HOMO–LUMO gap, which controls the second-order NLO response.

The role of ion pairing in tuning the second-order NLO response of cationic cyclometalated Ir^{III} complexes in CH_2Cl_2, and the effect of counterions and the concentration: Although it is known that ion-pairing plays an important role in tuning the structural properties and reactivity of transition-metal complexes,[12] the information on its influence on the second-order NLO properties of ionic complexes acting as second-order NLO chromophores is still limited. For instance, it has been reported that the second-order NLO response, measured by the hyper-Rayleigh scattering (HRS) technique in $CHCl_3$, of bimetallic cationic complexes (*E*)-$[CpFe(\eta^5\text{-}C_5H_4)(CH{=}CH)(C_6H_4)CNRuCp(PPh_3)_2]Y$ (Y = PF_6, BF_4) is dependent on the nature of the counterion. However, the extent of this ion pairing was unknown and considered quite negligible in $CHCl_3$.[13]

It was also reported that the quadratic hyperpolarizability, measured by the HRS technique in CH_2Cl_2, of the cationic complex with the ligand aryldiazovinylidene [Ru(C=CPhN=

NAr)(PPh$_3$)$_2$(η-C$_5$H$_5$)]Y (Y$^-$ = BF$_4^-$, Cl$^-$, Br$^-$, I$^-$, 4-MeC$_6$H$_4$SO$_3^-$, NO$_3^-$) is dependent on the nature of the counterion, its value increasing in the order Cl$^-$, Br$^-$, I$^-$ < 4-MeC$_6$H$_4$SO$_3^-$ < NO$_3^-$ < BF$_4^-$. Again the extent of ion pairing was unknown, but it was considered to be low or negligible; therefore the contributions of the cation and anion to the nonlinearity were considered largely independent.[14]

EFISH investigation: In the literature, there are only a few investigations on the use of the EFISH technique to determine the second-order NLO response of ionic species. This is because the migration of the dissociated ions under the applied external electric field could decrease the local field, thus impairing the solution second-order NLO response, unless a relatively low polar solvent, such as CHCl$_3$ or CH$_2$Cl$_2$, is used to stabilize ion-pairing.[15] In addition to our preliminary investigations on this new class of cyclometalated Ir^{III} complexes,[3–6] the $\mu\beta_{1.907}$ value of stilbazolium-like salts with I$^-$ as counterion was determined in CHCl$_3$,[16] whereas that involving various salts of cationic complexes, such as [η^5-C$_5$Me$_5$)Fe(η^6-C$_6$MeH$_5$)NHR][PF$_6$] (R = pyranylideneacetaldehyde hydrazone complexes)[17] and [η^5-C$_5$Me$_5$)Fe(η^6-C$_6$H$_5$)NHN=CHR][PF$_6$] (R = 2,4,6-Me$_3$C$_6$H$_2$; [(η^5-C$_5$H$_5$)Fe(η^5-C$_5$H$_4$)]) was recently determined in CH$_2$Cl$_2$.[18]

We now report that the nature of the counterion can control the absolute value of $\mu\beta_{1.907}$ in CH$_2$Cl$_2$ even if working at constant and similar concentration. For instance, for the cations **1a**, **1b**, **2a**, **2b**, **2e**, **2f**, and **5a**, the absolute value of $\mu\beta_{1.907}$ is lowered, when working in CH$_2$Cl$_2$ at a concentration of 10^{-3} M, by a factor of 0.6–0.8 upon substitution of PF$_6^-$ with C$_{12}$H$_{25}$SO$_3^-$ (Table 1).

This evidence prompted us to investigate in detail the effect of concentration, which can act on the extent of ion pairing and on the $\mu\beta_{1.907}$ value of the very efficient NLO chromophore **1b**-PF$_6$ (Table 2 and Figure 1). The absolute value of $\mu\beta_{1.907}$ in CH$_2$Cl$_2$ strongly increases on decreasing the concentration from 10^{-3} M down to about 10^{-4} M, reaching a value of about -5000×10^{-30} D cm^5 esu^{-1}. In contrast, the absolute value of $\mu\beta_{1.907}$ is not only lower, but also poorly sensitive to a decrease of the concentration if C$_{12}$H$_{25}$SO$_3^-$ or I$^-$ is substituted as the counterion (Figure 1). In fact, by decreasing the concentration from 10^{-3} M to 10^{-4} M, the $\mu\beta_{1.907}$ value for **1b**-C$_{12}$H$_{25}$SO$_3$ only increases from -1430 to -1770×10^{-30} D cm^5 esu^{-1}; and if I$^-$ is the counterion, the absolute value of $\mu\beta_{1.907}$ in CH$_2$Cl$_2$ is only slightly affected by the concentration (see **1b**-I in Table 2).

Table 2. EFISH $\mu\beta_{1.907}$ values ($\times10^{-30}$ D cm^5 esu^{-1}) of [Ir(ppy)$_2$(5-NO$_2$-1,10-phen)]Y measured in CH$_2$Cl$_2$ solution at various concentrations (C).

Y$^-$	$C = 1\times10^{-3}$ M	$C = 5\times10^{-4}$ M	$C = 1\times10^{-4}$ M
PF$_6^-$[a]	−2230	−2390	−4990
C$_{12}$H$_{25}$SO$_3^-$	−1430	−1520	−1770
I$^-$	−1160	−1370	−1370

[a] Values of -3670×10^{-30} and -5012×10^{-30} D cm^5 esu^{-1} were obtained by working with a concentration of 3×10^{-4} M and 5×10^{-5} M, respectively.

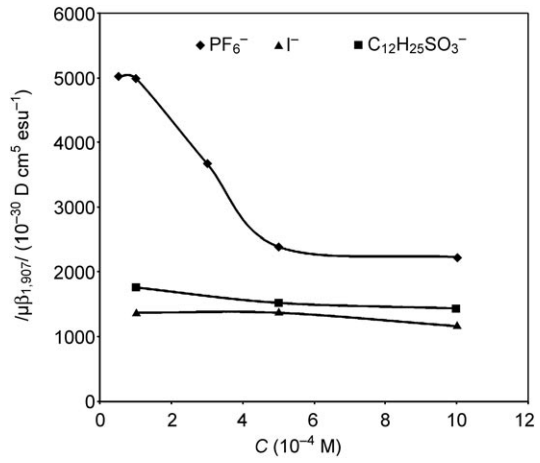

Figure 1. The effect of concentration in CH$_2$Cl$_2$ on the absolute value of $\mu\beta_{1.907}$ of **1b**-PF$_6$ ◆, **1b**-I ▲, and **1b**-C$_{12}$H$_{25}$SO$_3$ ■.

It seems, therefore, that the $\mu\beta_{1.907}$ absolute value is, in general, controlled by ion-pairing phenomena. Therefore, as the extent of a weak ion-pairing usually decreases with concentration, with a weakly interacting counterion of low polarizability such as PF$_6^-$, the value of $\mu\beta_{1.907}$ is concentration dependent and can reach high values. To confirm our qualitative preliminary observations by a more quantitative approach, we used pulsed field gradient spin-echo (PGSE) NMR spectroscopy to investigate the behavior of **1b**-PF$_6$, **1a**-PF$_6$, **3a**-PF$_6$, and **3b**-PF$_6$, in CH$_2$Cl$_2$ in the range of concentrations used for EFISH measurements.

NMR spectroscopic investigation: The relative orientation of the anion–cation and the fraction of dissociated ion pairs (α) as a function of the concentration were investigated for **1a**-PF$_6$, **1b**-PF$_6$, **3a**-PF$_6$, and **3b**-PF$_6$ working in CD$_2$Cl$_2$ by means of the nuclear Overhauser effect (NOE)[19] and PGSE[9] NMR experiments. The assignment of ^{1}H and ^{13}C resonances, propedeutic to NOE and PGSE studies, was performed by using multinuclear and multidimensional NMR spectroscopies (see Experimental Section).

All proton and carbon resonances belonging to 1,10-phenanthroline and to cyclometalated phenylpyridine (or phenylquinoline) ligands were easily grouped by their scalar and dipolar connectivity exhibited in ^{1}H, ^{13}C(J-modulated), ^{1}H-COSY, ^{1}H-NOESY, ^{1}H,^{13}C HMQC NMR, and ^{1}H,^{13}C HMBC NMR spectra (actually the two cyclometalated ligands are magnetically inequivalent, but their resonances are too close to be separated or, in some cases, they are coincident). The distinction between resonances of the two sides of the asymmetric phenanthroline ligand and of the two rings of the cyclometalated ligands was achieved by the observation of intra- and interligand key NOEs. For example, the evidence of an intra-ligand NOE between protons 7 (easily assigned being the only singlet) and 10 of the phenanthroline ligand leads to a complete assignment of the

phenanthroline resonances of **1b**-PF_6 (Figure 2). The interligand NOEs between protons 1 and 12 of the phenanthroline and two resonances at $\delta = 7.38$ ppm and 6.44 ppm, together with the known low-frequency shielding of the proton close to the σ-bonded carbon atom of a cyclometalated system,[20] allowed us to assign the latter signals to protons 13 and 22, respectively, of the cyclometalated ligand.

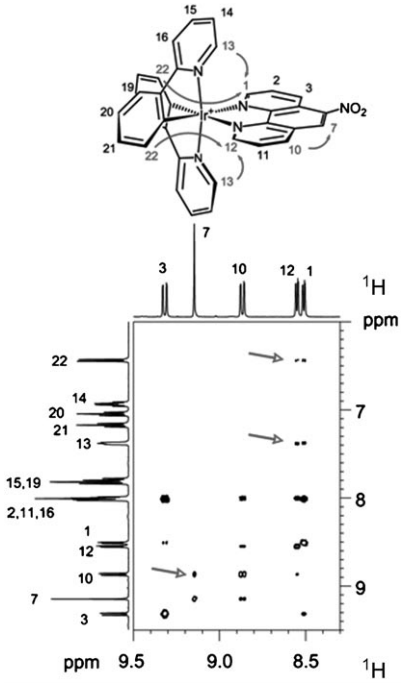

Figure 2. A section of the ^{1}H-NOESY NMR spectrum (400.13 MHz, 296 K, CD_2Cl_2) of **1b**-PF_6. Key NOEs are indicated with arrows.

Interionic NOE measurements: The relative orientation of the anion–cation in the case of **1a**-PF_6, **1b**-PF_6, **3a**-PF_6, and **3b**-PF_6 was investigated in CD_2Cl_2 by detecting dipolar interionic interactions in the ^{19}F,^{1}H-HOESY NMR spectrum. Strong NOE contacts were observed for **1b**-PF_6 between the F nuclei of the counterion PF_6^- and protons 7, 10, and 11 of 5-NO_2-1,10-phenanthroline and 13 and 14 protons of the pyridine ring of the cyclometalated ligand (Figure 3a). Very weak contacts were also found with proton 12 of the phenanthroline ligand, whereas no interaction of PF_6^- with other protons of the cyclometalated ligand and protons 1, 2 and 3 of the phenanthroline ligand was detected. The absence of NOEs with protons 1 of the phenanthroline and 15 of the cyclometalated ligand suggests that the interionic contacts evidenced between the counterion PF_6^- and the signals of the multiplet at $\delta = 8.00$ ppm (this latter accounting for protons 2, 11, and 16) is due only to proton 11. This pattern of NOE contacts indicates that the PF_6^- counterion is mainly located above and below the plane of the 5-NO_2-1,10-phenanthroline ligand on the other side with respect to the NO_2 substituent (Figure 3a, for the sake of simplicity only the position of PF_6^- below the phenanthroline plane is shown). Analysis of the ^{19}F,^{1}H-HOESY NMR spectrum of **1a**-PF_6 (Figure 3a) reveals strong contacts between the F

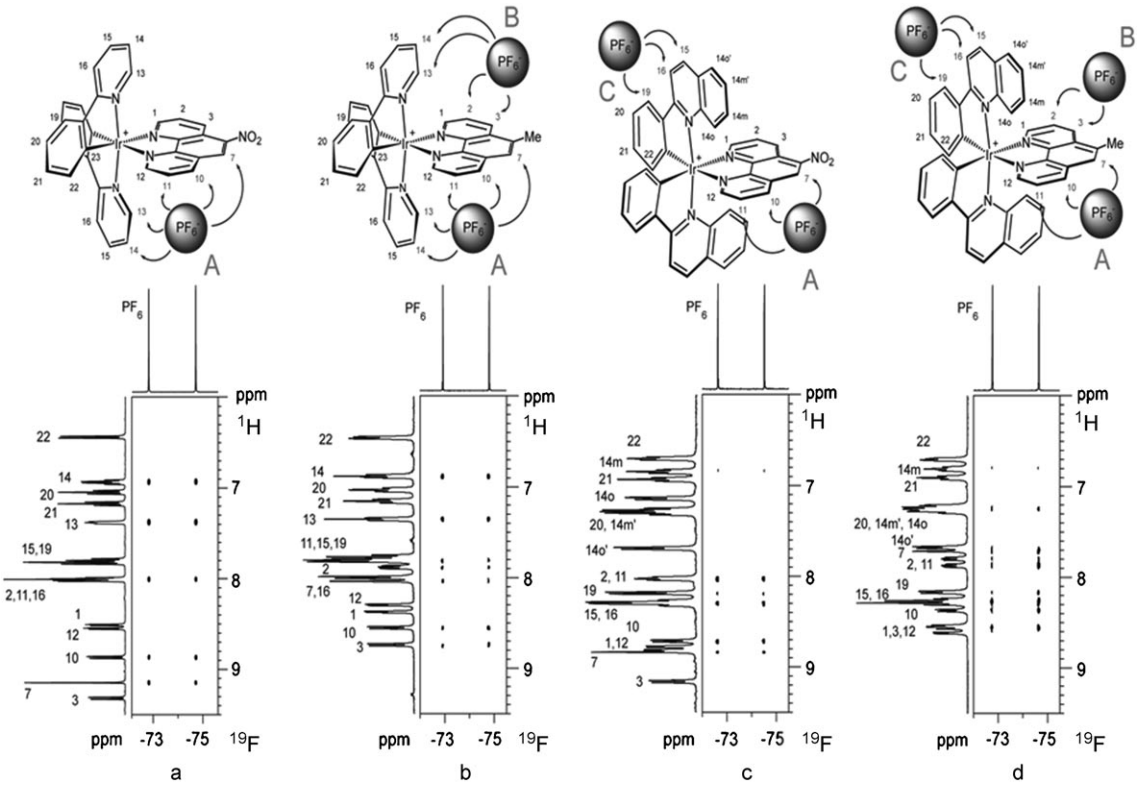

Figure 3. ^{19}F,^{1}H-HOESY NMR spectrum (376.65 MHz, 296 K, CD_2Cl_2) of a) **1b**-PF_6, b) **1a**-PF_6, c) **3b**-PF_6, and d) **3a**-PF_6.

nuclei of PF_6^- and all protons of the Me-substituted phenanthroline (protons 1, 2, 3, 7, 10, 11, 12 of phenanthroline and protons of the Me group; this latter group is not shown in Figure 3b) and only with protons 13 and 14 of the pyridine ring of the cyclometalated ligand. No interaction of PF_6^- could be detected with other protons of the cyclometalated ligand. Consequently, the counterion PF_6^- is still located above and below the plane of the phenanthroline system, but it approaches the asymmetric 5-Me-1,10-phenanthroline ligand from both sides (Figure 3b, for the sake of simplicity only the positions of the anion below the phenanthroline plane far from Me and above the phenanthroline plane close to the Me are shown). Strong contacts were observed between the F nuclei of PF_6^- and protons 10 and 11 of the 5-NO_2-1,10-phenanthroline in the $^{19}F,^1H$-HOESY NMR spectrum of **3b**-PF_6 (Figure 3c). Medium-intensity NOE contacts were observed with proton 7 of the phenanthroline and protons 15, 16, and 19 of the cyclometalated ligand. Very weak contacts were detected with proton 12 of the phenanthroline and 14m of the cyclometalated ligand. No interaction was detected with protons 22 of the cyclometalated ring and protons 1, 2, and 3 of the 5-NO_2-1,10-phenanthroline. This pattern of NOE contacts indicates that, as in **1b**-PF_6, the PF_6^- counterion is mainly located above and below the plane of the 5-NO_2-1,10-phenanthroline ligand, shifted on the other side with respect to the NO_2 substituent (the A position in Figure 3), but another orientation with the counterion on the side of the phenylquinoline system (the C position in Figure 3) is present as suggested by NOEs of the F nuclei of PF_6^- and protons 15,16,19 of the cyclometalated ligand (for the sake of simplicity only the positions of PF_6^- below the phenanthroline plane and close one phenylquinoline ligand are shown in Figure 3c). Although several resonances in the ^1H spectra of **3a**-PF_6 overlap, the interpretation of the $^{19}F,^1H$-HOESY, NMR data clearly indicate that orientations A, B, and C are present (Figure 3d, for the sake of simplicity only one of the two possible orientations of PF_6^- are shown for positions A, B, and C). In conclusion the highest degree of selective anion–cation interaction takes place in the case of **1b**-PF_6, caused by the electron withdrawing properties of the NO_2 substituent that leads to an asymmetric accumulation of negative charge on the side of the phenanthroline ligand carrying the NO_2 group. As a consequence, PF_6^- prefers to approach the cation from the opposite side. Such selective differentiation of the two sides of the asymmetric phenanthroline ligand is lost when -NO_2 is substituted by -Me (**1b**-PF_6→**1a**-PF_6). In this latter case the PF_6^- anion interacts mainly with the phenanthroline ligand, but it can equivalently locate in both sides with respect to the Me substituent. Finally, when phenylquinoline substitutes phenylpyridine, as the cyclometalated ligand (**1a**-PF_6→**3a**-PF_6; **1b**-PF_6→**3b**-PF_6), a placement of the PF_6^- counterion close to the phenylquinoline ligand (orientation C) occurs as well and becomes competitive, although at less extent, with the interaction with the phenanthroline system (orientations A and B).

PGSE measurements: ^1H and ^{19}F PGSE NMR experiments were carried out for **1a**-PF_6, **1b**-PF_6, **1b**-$C_{12}H_{25}SO_3$ **3a**-PF_6, and **3b**-PF_6 in CD_2Cl_2 by using tetrakis(trimethylsilyl)silane (TMSS), as internal standard (see the Experimental Section for details). PGSE measurements allow the translational self-diffusion coefficients (D_t) for both cationic (D_t^+) and anionic (D_t) components of the ion pair to be determined (Table 3). From the measured self-diffusion coefficients (D_t), the average hydrodynamic radius (r_H) of the diffusing species were derived by the Stokes–Einstein Equation (2):

$$D_t = \frac{kT}{c\pi\eta r_H} \quad (2)$$

in which k is the Boltzman constant, T is the temperature, c is a numerical factor and η is the solution viscosity (Table 3). D_t experimental data were treated taking all the methodological precautions recently described.[21,22] From the average hydrodynamic radii of the diffusing ionic species, determined experimentally and assumed to be spherical, their volumes (V_H^+ and V_H^-) were obtained (Table 3).

To evaluate the average level of aggregation in solution, the values of V_H^+ and V_H^- were compared with the hydrodynamic volume of the ion pair V_H^{ip}, calculated as the addition of the calculated hydrodynamic volume of the cation (V_H^{0+}) and that of the anion (V_H^{0-}). As V_{VdW} (Van der

Table 3. Diffusion coefficients ($10^{10}\,D_t\,m^2s^{-1}$), hydrodynamic radius (r_H, Å), hydrodynamic volume (V_H, Å^3) and fraction of dissociated ion-pairs (α) in CD_2Cl_2 for **1a**-PF_6, **1b**-PF_6, **1b**-$C_{12}H_{25}SO_3$ **3a**-PF_6, and **3b**-PF_6, as a function of concentration (C, mM).

		D_t^+	D_t^-	r_H^+	r_H^-	V_H^+	V_H^-	α	C
1	**1a**-PF_6	9.1	12.1	6.1	4.9	946	487	0.55	4.0
2	**1a**-PF_6	8.9	11.7	6.2	5.0	1017	539	0.53	12.0
3	**1a**-PF_6	8.7	11.4	6.4	5.2	1092	596	0.51	25.0
4	**1b**-PF_6	9.2	16.4	6.04	3.90	922	248	0.80	0.03
5	**1b**-PF_6	9.1	15.1	6.08	4.13	941	295	0.75	0.08
6	**1b**-PF_6	8.9	12.1	6.17	4.79	983	460	0.59	0.60
7	**1b**-PF_6	8.9	11.4	6.10	5.01	950	526	0.50	1.20
8	**1b**-PF_6	8.5	10.2	6.35	5.45	1072	678	0.42	9.50
9	**1b**-PF_6	8.0	9.5	6.49	5.60	1145	735	0.41	16.0[a]
10	**1b**-$C_{12}H_{25}SO_3$	8.2	8.2	6.60	6.59	1204	1198	$\leq$0.05	0.99
11	**1b**-$C_{12}H_{25}SO_3$	8.0	8.0	6.71	6.69	1265	1254	$\leq$0.05	1.89
12	**3a**-PF_6	8.5	12.0	6.4	4.8	1129	478	0.64	3.0
13	**3a**-PF_6	8.4	12.0	6.5	4.9	1160	483	0.63	10.0
14	**3a**-PF_6	8.1	11.2	6.6	5.0	1177	526	0.61	25.0
15	**3b**-PF_6	8.3	12.3	6.6	4.8	1193	458	0.67	2.0
16	**3b**-PF_6	8.1	10.7	6.6	5.2	1204	610	0.54	12.0
17	**3b**-PF_6	7.6	9.6	6.9	5.7	1412	759	0.51	25.0

[a] Saturated solution.

Walls volume) well-describes the hydrodynamic volume V_H for molecules approaching a spherical shape that do not possess inlets, V_{vdW} (70 Å^3) was taken as V_H^{0-} for the counterion PF_6^-, whereas V_H^{0+} (908 Å^3 for **1a** and **1b**, 1103 Å^3 for **3a** and **3b**) and V_H^{0-} for $C_{12}H_{25}SO_3^-$ (346 Å^3) were calculated starting from the molecular structures by the approach recently described.[23]

From Table 3 it can be noted that the value of V_H^+ oscillates between V_H^{0+} and V_H^{IP} (in some cases it even exceeds V_H^{IP}), whereas the value of V_H^- is always included between V_H^{0-} and V_H^{IP}. The fractions (α in Table 3) of ions, ion pairs, and ion quadruples (necessary to account for the slightly higher value of V_H^+ with respect to V_H^{IP}) were calculated with the assumption that only dissociated ion pairs, ion pairs, and ion quadruples were present in CH_2Cl_2 solution.[24] The value of α ranges from 0.80 (3×10^{-5} M) to 0.40 (saturated solution, 16×10^{-3} M) for **1b**-PF_6, whereas **1b**-$C_{12}H_{25}SO_3$ shows only marginal dissociation ($\alpha \leq 0.05$) in all the range of the concentrations investigated, confirming the stronger tendency to form ion pairing of the $C_{12}H_{25}SO_3^-$ counterion when compared to PF_6^-. Some other trends can be deduced from Table 3. The dissociation of the ion pair increases slightly by i) substituting the NO_2 group with the Me group on the phenanthroline ligand (compare in Table 3 entries 2 and 3 with entries 8 and 9, respectively, and entries 13 and 14 with entries 16 and 17, respectively). ii) Changing the phenylpyridine ligands with the phenylquinoline ones (compare in Table 3 entries 2 and 3 with 13 and 14, respectively and entries 8 and 9 with 16 and 17, respectively). Both trends are expected since i) a minor charge polarization is expected when the NO_2 group is replaced by the Me group, which renders the cation least attracting for the counterion and, consequently, reduces the strength of ion pairing and ii) the size of the cation is higher for **3a**, **3b** when compared to **1a**, **1b** so that the tendency to form ion pairs is expected to be reduced.

In the case of **1b**-PF_6, a clear correlation between the dependence on concentration of the absolute values of $\mu\beta_{1.907}$ and α can be sketched from data reported in Tables 2 and 3 (Figure 4). Dilution causes a relevant increase of the dissociated ion pair causing in parallel a strong increase of the absolute value of $\mu\beta_{1.907}$. Such a direct correlation between the increase of the concentration of dissociated species and the increase of the second-order NLO response was already reported by some of us in the case of solvolysis in $CHCl_3$ of some stilbazolic Zn^{II} complexes with sulfonated ancillary ligands.[1h]

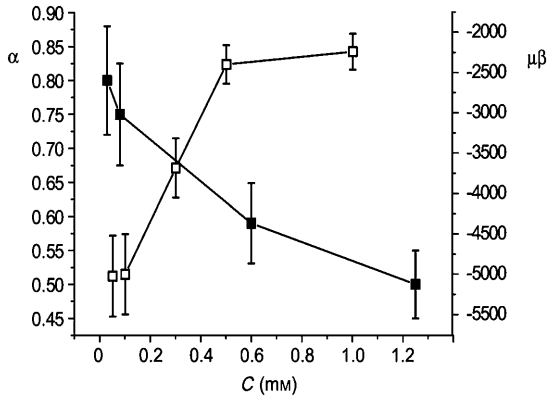

Figure 4. α (■) and absolute value of $\mu\beta_{1.907}$ ($\times10^{-30}$ D cm^5 esu^{-1}, □) for **1b**PF_6 in CH_2Cl_2 at different concentrations.

Theoretical investigation of the ion pairing and its effects on the electronic structure: To provide insight into the effect of ion pairing on the structural, electronic, and second order NLO properties of the cationic Ir^{III} NLO chromophores investigated in this work, we performed DFT and TDDFT comparative calculations[11] (see the Experimental Section) on both the **1b** cation, $[Ir(ppy)_2(5\text{-}NO_2\text{-}1,10\text{-phen})]^+$, and its ion-pair with PF_6^- taking into account also solvation effects in CH_2Cl_2 solution. Several different mutual arrangements of the cation and anion in the ion-pair structure were investigated, followed by full-geometry optimization. A minimum energy for the structure of the ion pair was found with the PF_6^- anion localized above the plane of the phenanthroline ligand, with a shortest contact distance of 2.74 Å between PF_6^- and the plane. Such localization of the PF_6^- anion with respect to the asymmetric structure of the phenanthroline is perfectly consistent with that found by means of $^{19}F,^1H$ HOESY NMR spectroscopy (Figure 3). This ion-pair configuration was retained for the subsequent TDDFT calculations.

The optimized molecular structure of the Ir^{III} complex is only slightly affected by the formation of the ion-pair, the most noticeable effect being a slight distortion from the planar geometry of the 5-NO_2-1,10-phenanthroline ligand. The comparison between the frontier molecular orbitals of the cation and its ion-pair with PF_6^- are reported in Figure 5, together with isodensity plots of selected molecular orbitals for the latter. The basic electronic structure of the cation is maintained also for the ion-pair, since the PF_6^- counterion does not affect the overall character of the frontier molecular orbitals, whereas some significant differences are found on the energy levels. In particular, aligning the HOMO energies to the same value, ion pairing produces a destabilization of the LUMOs set relative to the HOMOs, due to the perturbation exerted by PF_6^- on the π^* orbitals of the phenanthroline ligand. Overall, the HOMO–LUMO gap increases, passing from 2.07 eV for the cation to 2.20 eV for the ion-pair with PF_6^- (Figure 5). Besides, calculations show that that although in the cation the dipole moment is roughly aligned along the metal–phenanthroline axis, the presence of the PF_6^- counterion introduces a significant component along the direction connecting the PF_6^- anion and the Ir^{III} center.

The absorption spectrum of the cation $[Ir(ppy)_2(5\text{-}NO_2\text{-}1,10\text{-phen})]^+$ and of its ion-pair with PF_6^- was computed by determining the lowest 90 excited states, up to 220 nm, by TDDFT. The computed absorption spectra for the cation and the ion-pair are as expected similar, but show appreciable variations in the position and intensity of the low energy

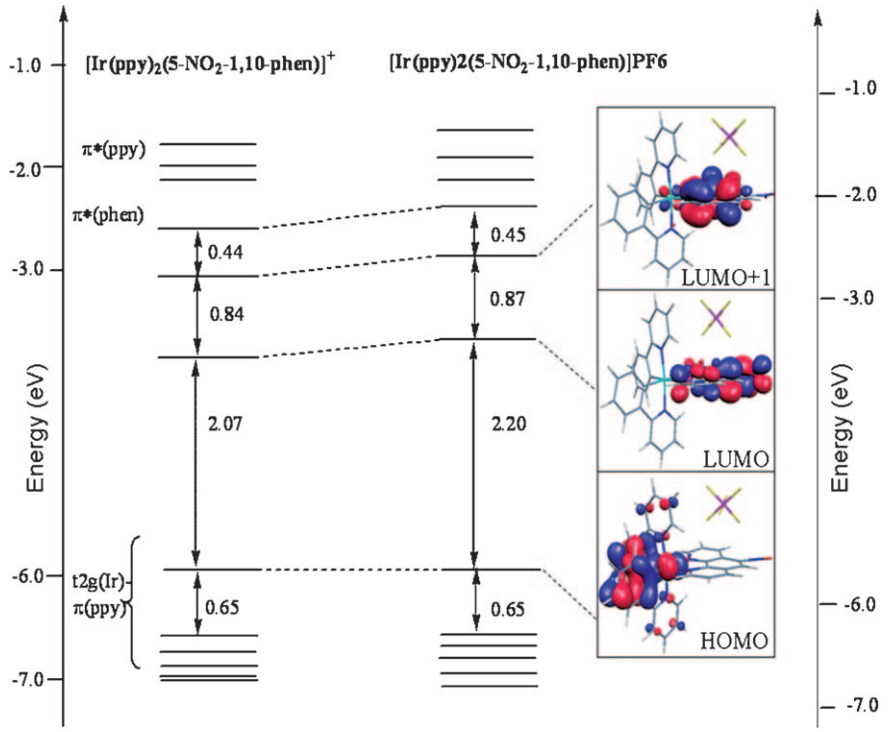

Figure 5. Energy and character of the frontier molecular orbitals of $[Ir(ppy)_2(5\text{-}NO_2\text{-}1,10\text{-}phen)]^+$ and of $[Ir(ppy)_2(5\text{-}NO_2\text{-}1,10\text{-}phen)]PF_6$. The energy scales have been aligned so that the energy of the HOMO may coincide (notice the different scale on the left and right panels).

bands related to HOMO–LUMO transitions at about 330–400 nm (Figure 6), in line with the perturbation exerted by the PF_6^- anion on the LUMO levels. The SOS investigation of the second order NLO response performed for the ion-pair revealed that, also in the ion-pair the charge transfer transitions from the $Ir(t_{2g})$-ppy(π) HOMO to the π^* LUMO and LUMO+1 levels of the phenanthroline ligand, which dominate the low energy portion of the absorption spectrum (Figure 6), are still those mainly affecting the value of the EFISH hyperpolarizability. Most notably, a decrease of the absolute value of the EFISH molecular hyperpolarizability was calculated by shifting from the cation to its ion-pair, although maintaining the same sign. Such a decrease, is clearly related to the opening of the HOMO–LUMO gap , which produces MLCT excitations of higher energy, which in turn should lead to a reduced second order NLO response, as expected on the basis of the two-level model.[7b]

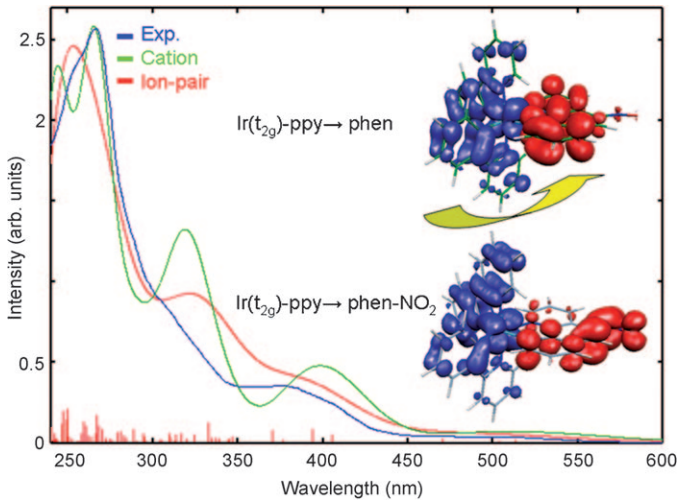

Figure 6. Comparison between the experimental (10^{-5} M in CH_2Cl_2, blue line) and calculated absorption spectra in CH_2Cl_2 solution for $[Ir(ppy)_2(5\text{-}NO_2\text{-}1,10\text{-}phen)]^+$ (green line) and for its ion-pair $[Ir(ppy)_2(5\text{-}NO_2\text{-}1,10\text{-}phen)][PF_6]$ (red line). Also shown is a charge density difference between selected MLCT excited states and the ground state for two low-lying charge transfer transitions: a blue (red) color indicates a decrease (increase) of the electron density upon excitation.

However, since the EFISH measurements give only the $\mu\beta_{1.907}$ value, where $\beta_{1.907}$ is the projection of the vector component β_{vec} along the dipole moment vector, a comparative analysis of the origin of the difference between the absolute values of $\mu\beta_{1.907}$ of the cation and its ion pair can not be done, since both the absolute value and the orientation of the dipole moment are affected by ion pairing and not only the value of the quadratic hyperpolarizability. Therefore from our theoretical investigation we can only suggest that ion pairing should produce a lowering of $\beta_{1.907}$. The effect on the value of the dipole moment is not so clear since it is difficult to define a precise dipole moment for cationic species.

Conclusion

We have presented in this work a full investigation on the second order NLO response, measured by the EFISH technique as $\mu\beta_{1.907}$ (see the Experimental Section) of a new class of cationic organometallic cyclometalated Ir^{III} NLO chromophores. By analysis of the role of the substituents on the 1,10-phenanthroline ligand, of the nature of the cyclometalated ligands and of the concentration and nature of the counterion, we evidenced the many different features controlling the EFISH second order NLO response of these NLO chromophores.

Based on DFT and TDDFT calculations, it appears that the EFISH quadratic hyperpolarizability is controlled by HOMO–LUMO MLCT transitions involving the metal-cy-

clometalated ligand as the donor and the 1,10-phenanthroline π* system as the acceptor. Therefore, the second order NLO response can be modulated and tuned in a reasonable way by controlling independently the nature of the substituents on the 1,10-phenanthroline ligand and the choice of the cyclometalated ligands. Moreover we have shown that ion pairing can affect the absolute value of $\mu\beta_{1.907}$, obtained by EFISH measurements, and can produce, when the ion pair is not too tight, a significant increase of such absolute value by dilution in CH_2Cl_2 solution with parallel decrease of the extent of ion pairing as supported by the PGSE NMR measurements. Since in the EFISH technique a dc electric field of about 30000 $V\,cm^{-1}$ is used, such correlation could not be real if due to an enhancement of ion pair dissociation induced by the electric field.[25] However, calculations completed by using a mathematical expression developed by Onsager[26] have shown that the effect of such a strong dc electric field on the dissociation of an ion pair (like that of **1b**-PF_6) is quite irrelevant,[27] so that the correlation between PGSE and EFISH experiments is quite reliable. We cannot however exclude the presence of a loosely bound long-ranged ion-pair, stabilized by the electric field.

Besides a thorough investigation of the effect of different counterions ($C_{12}H_{25}SO_3^-$, I^-, or PF_6^-) and of the concentration on the absolute value of $\mu\beta_{1.907}$ of some of these cationic NLO chomophores, by a combination of EFISH and ^1H and ^{19}F pulsed field gradient spin-echo (PGSE) NMR techniques together with DFT/TDDFT calculations, have provided some insight into the electronic modifications introduced by ion pairing and their effects on the absolute values of $\mu\beta_{1.907}$, taken as a measure of the second order NLO response.

The origin of the increased absolute values of $\mu\beta_{1.907}$ by dilution in CH_2Cl_2 can be partly attributed to the decrease of the electronic perturbation induced by the counterion on the LUMO levels of the cyclometalated Ir^{III} NLO chromophore. This point is confirmed by the strong dependence of the absolute values of $\mu\beta_{1.907}$ on the nature of the counterion, being lower for the strong ion-pairing. Notably, the preliminary investigations show that the β_{HLS} value, measured by the hyper-Rayleigh scattering technique in CH_2Cl_2 of **1b** is also dependent on the nature of the counterion.[28] Remarkably, upon substitution of the PF_6^- ion by $C_{12}H_{25}SO_3^-$, the value of β_{HLS} decreases by a factor of about 0.65 similar to the decrease observed for the value of EFISH $\mu\beta_{1.907}$. A contribution to the increased EFISH $\mu\beta_{1.907}$ observed here, might also arise from the increased dipole moment of the above-mentioned loose-ion pair.

In conclusion, ion pairing exerts, in CH_2Cl_2 solution, a significant influence on the value of EFISH $\mu\beta_{1.907}$ of this new class of cationic Ir^{III} NLO chromophores, a factor that should be definitely taken into careful account.

Experimental Section

General comments: All reagents and solvents were purchased from Sigma–Aldrich, except $IrCl_3$ hydrate, which was purchased from Engelhard. Complexes as PF_6^- salts were prepared as previously reported,[2–6] whereas those with $C_{12}H_{25}SO_3^-$ or I^- as counterion were prepared in a similar manner, but using $Na[C_{12}H_{25}SO_3]$ and KI, respectively, instead of $[NH_4][PF_6]$, as described below in the case of **1b**-I and **1b**-$C_{12}H_{25}SO_3$. All reactions were carried out under nitrogen. Products were characterized by using ^1H NMR (Bruker Avance DRX-400 instrument), UV/visible (Jasco V-570 spectrometer),and elemental analyses.

Synthesis of cyclometalated Ir^{III} complexes

*[Ir(ppy)$_2$(5-NO$_2$-1,10-phen)]I (**1b-I**)*: A solution of $[Ir(ppy)_2Cl]_2$ and 5-NO_2-1,10-phen in CH_2Cl_2/MeOH (15 mL, 2:1 v/v) was heated under reflux. After 5–6 h, the orange solution was cooled to room temperature, and then a 10-fold excess of potassium iodide was added. The suspension was stirred for 15 min and then filtered to remove insoluble inorganic salts. The solution was evaporated to dryness under reduced pressure to obtain a crude orange solid. The solid was dissolved in CH_2Cl_2 and filtered to remove the residual traces of inorganic salts. Diethyl ether was layered onto the orange filtrate, and the mixture was cooled to about 0°C. Orange plates of the desired product formed overnight. Yield: 0.0916 g (72%, starting from 0.0800 g, 0.0746 mmol of $[\{Ir(ppy)_2Cl\}_2]$). Elemental analysis calcd (%) for $IrC_{34}H_{23}N_5IO_2$: C 47.89, H 2.72 N, 8.21; found: C 47.22, H 2.65, N 8.34%.

*[Ir(ppy)$_2$(5-NO$_2$-1,10-phen)][C$_{12}$H$_{25}$SO$_3$] (**1b**-C$_{12}$H$_{25}$SO$_3$)*: A solution of $[\{Ir(ppy)_2Cl\}_2]$ and 5-NO_2-1,10-phen in CH_2Cl_2/MeOH (15 mL, 2/1 v/v) was heated under reflux. After 5–6 h, the orange solution was cooled to room temperature, and then a 10-fold excess of sodium dodecansulfonate was added. The suspension was stirred for 15 min and then filtered to remove insoluble inorganic salts. The solution was evaporated to dryness under reduced pressure to obtain a crude orange solid. The solid was dissolved in CH_2Cl_2 and filtered to remove the residual traces of inorganic salts. Diethyl ether was layered onto the orange filtrate, and the mixture was cooled to about 0°C. Orange plates of the desired product formed overnight. Yield: 0.1113 g (68%, starting from 0.0900 g, 0.0839 mmol of $[\{Ir(ppy)_2Cl\}_2]$). Elemental analysis calcd (%) for $IrC_{46}H_{48}N_5SO_5$: C 56.66, H 4.96, N 7.18; found: C 57.01, H 4.88, N 7.05.

*[Ir(ppy)$_2$(5-Me-1,10-phen)][C$_{12}$H$_{25}$SO$_3$] (**1a**-C$_{12}$H$_{25}$SO$_3$)*: The complex was obtained in 67% yield, starting from $[\{Ir(ppy)_2Cl\}_2]$ and 5-Me-1,10-phen, following a procedure similar to that of **1b**-$C_{12}H_{25}SO_3$. Elemental analysis calcd (%) for $IrC_{47}H_{51}N_4SO_3$: C 59.79, H 5.44, N 5.93; found: C 58.60, H 5.55, N 5.23.

*[Ir(dpmt)$_2$(5-Me-1,10-phen)][C$_{12}$H$_{25}$SO$_3$]. (**5a**-C$_{12}$H$_{25}$SO$_3$)*: The complex was obtained in 74% yield, starting from $[\{Ir(dpmt)_2Cl\}_2]$ and 5-Me-1,10-phen, following a procedure similar to that of **1b**-$C_{12}H_{25}SO_3$. Elemental analysis calcd (%) for $IrC_{56}H_{59}N_4S_3O_3$: C 59.04, H 5.23, N 4.93; found: C 58.71, H 5.14, N 4.62.

EFISH measurements: All EFISH measurements[7] were carried out at the Dipartimento di Chimica Inorganica Metallorganica e Analitica "Lamberto Malatesta" of the Università di Milano, in CH_2Cl_2 solutions of different concentrations (10^{-3} M, 5×10^{-4} M, 3×10^{-4} M, 10^{-4} M, and 5×10^{-5} M) working with a non resonant incident wavelength of 1.907 μm, obtained by Raman-shifting the fundamental 1.064 μm wavelength produced by a Q-switched, mode-locked Nd^{3+}:YAG laser manufactured by Atalaser. The apparatus for the EFISH measurements was made by SOPRA (France).

NOE and PGSE experiments: One- and two-dimensional ^1H, ^{13}C, ^{19}F, and ^{31}P NMR spectra of **1a**-PF_6, **1b**-PF_6, **3a**-PF_6, and **3b**-PF_6 were measured by using Bruker DRX 400 spectrometers. Referencing is relative to TMS (^1H and ^{13}C), CCl_3F(^{19}F), and 85% H_3PO_4 (^{31}P). NMR samples were prepared dissolving the suitable amount of compound in CD_2Cl_2 (0.5 mL). The ^1H-NOESY[29] NMR experiments were acquired by the standard three-pulse sequence or by the PFG version.[30] Two-dimensional ^{19}F,^1H-HOESY NMR experiments were acquired using the standard four-pulse sequence or the modified version.[31] The number of transients and the number of data points were chosen according to the sample concentration and to the desired final digital resolution. Semi-quantitative spectra were acquired using a 2 s relaxation delay and 800 ms mixing times. The numbering of carbon and proton resonances is illustrated in Scheme 2.

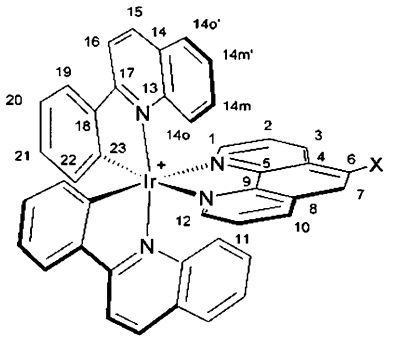

Scheme 2. Numbering scheme for carbon and proton resonances.

NMR data for **1b**-PF_6 ^{1}H NMR (CD_2Cl_2, 298 K, 400.13 MHz): δ = 6.44 (dd, $^3J_{22-21}$ = 7.3, $^4J_{22-20}$ = 1.0 Hz, 22), 6.93 (m, 14), 7.04 (dd, $^3J_{20-21}$ = $^3J_{20-19}$ = 7.5, 20 Hz), 7.17 (dd, $^3J_{21-20}$ = $^3J_{21-22}$ = 7.5, 21 Hz), 7.38 (m, 13), 7.82 (m, 15 and 19), 8.00 (m, 2, 11 and 16), 8.51 (dd, $^3J_{1-2}$ = 5.0 Hz, $^4J_{1-3}$ = 1.4 Hz, 1), 8.55 (dd, $^3J_{12-11}$ = 5.2 Hz, $^4J_{12-10}$ = 1.4 Hz, 12), 8.87 (dd, $^3J_{10-11}$ = 8.3, $^4J_{10-12}$ = 1.4 Hz, 10), 9.15 (s, 7), 9.32 ppm (dd, $^3J_{3-2}$ = 8.7, $^4J_{3-1}$ = 1.4 Hz, 3); $^{13}C\{^1H\}$-NMR (CD_2Cl_2, 298 K): δ = 120.4 (s, C16), 123.5 (s,C21), 123.9 and 124.0 (s,14), 124.9 (s,6), 125.4 (s,19), 127.7 (s,7), 128.4 and 128.5 (s, 2 and 11), 129.0 (s,9), 131.2 (s,20), 132.1 (s,22), 135.7 (s,3), 138.8 (s,15), 140.8 (s,10), 144.1 and 144.2 (s,23 and 23′), 145.6 (s,4), 147.7 (s,5), 148.6 (s,8 or 18) , 148.7 (s,8 or 18), 149.0 and 149.1 (s, 13 and 13′), 152.9 (s,1), 154.5 (s,12), 168.0 ppm (s,17); ^{19}F NMR (CD_2Cl_2, 298 K): δ = −74.2 ppm (d, $^1J_{FP}$ = 711 Hz); ^{31}P NMR (CD_2Cl_2, 298 K): δ = −143.2 ppm (sept, $^1J_{PF}$ = 711 Hz).

NMR data for **1a**-PF_6 ^{1}H NMR (CD_2Cl_2, 298 K, 400.13 MHz): δ = 2.95 (s, Me), 6.45 (dd, $^3J_{22-21}$ = 7.3, $^4J_{22-20}$ = 1.0 Hz, 22), 6.88 (m, 14), 7.03 (dd, $^3J_{20-21}$ = $^3J_{20-19}$ = 7.5 Hz, 20), 7.15 (dd, $^3J_{21-20}$ = $^3J_{21-22}$ = 7.5 Hz, 21), 7.35 (m, 13), 7.77 (m, 15 and 19), 7.81 (m, 11), 7.88 (m, 2), 7.99 (d, $^3J_{16-15}$ = 8.5 Hz, 16), 8.04 (s, 7), 8.30 (d, $^3J_{12-11}$ = 5.0 Hz, 12), 8.37 (d, $^3J_{1-2}$ = 5.2 Hz, 1), 8.55(d, $^3J_{10-11}$ = 8.5 Hz, 10), 8.73 ppm (dd, $^3J_{3-2}$ = 8.5 Hz, 3); ^{19}F NMR (CD_2Cl_2, 298 K): δ = −74.2 ppm (d, $^1J_{FP}$ = 711 Hz); ^{31}P NMR (CD_2Cl_2, 298 K): δ = −143.2 ppm (sept, $^1J_{PF}$ = 711 Hz).

NMR data for **3b**-PF_6 ^{1}H NMR (CD_2Cl_2, 298 K, 400.13 MHz): δ = 6.70 (m, 22), 6.84 (dd, $^3J_{14m-14o}$ = $^3J_{14m-14m'}$ = 7.6, 14 m), 6.93 (dd, $^3J_{21-22}$ = $^3J_{21-20}$ = 7.6, 21), 7.14 (d, $^3J_{14o-14m}$ = 8.4, 14o), 7.29 (m, 20 and 14 m′), 7.69 (d, $^3J_{14o'-14m'}$ = 8.0, 14o′), 8.03 (m, 2 and 11), 8.19 (d, $^3J_{19-20}$ = 8.4, 19), 8.29 (m, 15 and 16), 8.71 (d, $^3J_{10-11}$ = 8.3, 10), 8.78 and 8.81(d, $^3J_{1(12)-2(11)}$ = 5.0, 1 and 12), 8.83 (s, 7), 9.19 ppm (d, $^3J_{3-2}$ = 8.7, 3); ^{19}F NMR (CD_2Cl_2, 298 K): δ = −74.2 ppm (d, $^1J_{FP}$ = 711); ^{31}P NMR (CD_2Cl_2, 298 K): δ = −143.2 ppm (sept, $^1J_{PF}$ = 711).

NMR data for **3**a-PF_6 ^{1}H NMR (CD_2Cl_2, 298 K, 400.13 MHz, *J* in Hz): δ = 2.72 (s, Me), 6.70 (m, 22), 6.80 (dd, $^3J_{14m-14o}$ = $^3J_{14m-14m'}$ = 7.6 Hz, 14 m), 6.91 (dd, $^3J_{21-22}$ = $^3J_{21-20}$ = 7.6 Hz, 21), 7.24 (m, 20, 14 m′ and 14o), 7.67 (d, $^3J_{14o'-14m'}$ = 8.1 Hz, 14o′), 7.71 (s, 7), 7.79 and 7.87 (d, $^3J_{2(11)-1(12)}$ = 5.0 Hz, 2 and 11), 8.16 (d, $^3J_{19-20}$ = 8.4 Hz, 19), 8.26 (m, 15 and 16), 8.37 (d, $^3J_{10-11}$ = 8.3 Hz, 10), 8.57 ppm (m, 1,3 and 12); ^{19}F NMR (CD_2Cl_2, 298 K): δ = −74.2 ppm (d, $^1J_{FP}$ = 711 Hz); ^{31}P NMR (CD_2Cl_2, 298 K): δ = −143.2 ppm (sept, $^1J_{PF}$ = 711 Hz).

All the PGSE NMR measurements were performed by means of the standard stimulated echo pulse sequence[32] available by using a Bruker AVANCE DRX 400 spectrometer equipped with a GREAT 1/10 gradient unit and a QNP probe with a Z-gradient coil, at 296 K without spinning.

The dependence of the resonance intensity (*I*) on a constant waiting time and on a varied gradient strength (*G*) is described by Equation (3):

$$\ln\frac{I}{I_0} = -(\gamma\delta)^2 D_t\left(\Delta - \frac{\delta}{3}\right)G^2 \qquad (3)$$

in which *I* = intensity of the observed spin echo, I_0 = intensity of the spin echo without gradients, D_t = diffusion coefficient, Δ = delay between the midpoints of the gradients, δ = length of the gradient pulse, and γ = magnetogyric ratio.

The shape of the gradients was rectangular, their duration (δ) was 4–5 ms, and their strength (*G*) was varied during the experiments. The semi-logarithmic plots of $\ln(I/I_0)$ versus G^2 were fitted using a standard linear regression algorithm and an *R* factor better than 0.99 was always obtained. Different values of Δ, "nt" (number of transients) and number of different gradient strengths (*G*) were used for different samples.

The self-diffusion coefficient D_t, that is directly proportional to the slope of the regression line obtained by plotting $\log(I/I_o)$ versus G^2 [Eq. (3)], was estimated by measuring the proportionality constant, using a sample of HDO (5%) in D_2O (known diffusion coefficient in the range 274–318 K)[33] in the same exact condition as the sample of interest using TMS as internal standard. D_t data were treated as described in the literature.[19–24]

The measurement uncertainty was estimated by determining the standard deviation of *m* by performing experiments with different Δ values. Standard propagation of error analysis yielded a standard deviation of approximately 3–4% in the hydrodynamic radius and 10% in the hydrodynamic volumes and α.

Theoretical calculations: The structures, as in the results discussed below, were optimized by using the BP86 exchange-correlation function,[34] together with a TZP (DZP) basis set for Ir (N, C, O, H), including scalar-relativistic corrections as implemented in the ADF program.[35] On the optimized geometries, single point calculations were performed with the Gaussian03 program package[36] at the B3LYP/LANL2DZ level,[37,38] including solvation effects by PCM.[39] The computed optimized molecular structures maintain the same basic skeleton, retrieving a very good agreement with structural X-ray data.[2c,3–5] The projection of the static quadratic hyperpolarizability tensor along the dipole moment has been computed by the sum over states approach (SOS),[40] based on explicit calculation of two-level terms for the lowest 80–100 excited states, as preliminary reported,[3] thus affording the contribution of each excited state to the static EFISH quadratic hyperpolarizability.

Acknowledgements

We deeply thank Prof. Isabelle Ledoux-Rak (Ecole Normale Supérieure de Cachan, France) for fruitful discussions and Dr. Elisa Tordin for some EFISH measurements. This work was supported by MIUR (FIRB 2003: Molecular compounds and hybrid nanostructured materials with resonant and non resonant optical properties for photonic devices and PRIN 2007: Nuove strategie per il controllo di reazioni metallo assistite: interazioni non convenzionali di frammenti molecolari) and by CNR (PROMO 2006: Sistemi molecolari e nanodimensionali con proprietà funzionali: Nanostrutture organiche, organometalliche, polimeriche ed ibride; ingegnerizzazione supramolecolare delle proprietà fotoniche e dispositivistica innovativa per optoelettronica).

[1] For example, see a) D. R. Kanis, P. G. Lacroix, M. A. Ratner, T. J. Marks, *J. Am. Chem. Soc.* **1994**, *116*, 10089; b) J. Heck, S. Dabek, T. Meyer-Friedrichsen, H. Wong, *Coord. Chem. Rev.* **1999**, *190–192*, 1217; c) H. Le Bozec, T. Renouard, *Eur. J. Inorg. Chem.* **2000**, 229; d) P. G. Lacroix, *Eur. J. Inorg. Chem.* **2001**, 339; e) S. Di Bella, *Chem. Soc. Rev.* **2001**, *30*, 355; f) B. J. Coe in *Comprehensive Coordination Chemistry II, Vol. 9* (Eds.: J. A. McCleverty, T. J. Meyer), Elsevier, Oxford, **2004**, pp. 621–687; g) B. J. Coe, N. R. M. Curati, *Comments Inorg. Chem.* **2004**, *25*, 147; h) E. Cariati, M. Pizzotti, D. Roberto, F. Tessore, R. Ugo, *Coord. Chem. Rev.* **2006**, *250*, 1210; i) B. J. Coe, *Acc. Chem. Res.* **2006**, *39*, 383; j) M. G. Humphrey, M. Samoc, *Adv. Organomet. Chem.* **2008**, *55*, 61.

[2] For example, see a) Q. Zhao, S. Liu, M. Shi, C. Wang, M. Yu, L. Li, F. Li, T. Yi and C. Huang, *Inorg. Chem.* **2006**, *45*, 6152; b) H. J. Bolink, L. Cappelli, E. Coronado, M. Grätzel, E. Ortì, R. D. Costa, P. M. Viruela, M. K. Nazeeruddin, *J. Am. Chem. Soc.* **2006**, *128*, 14787; c) C. Dragonetti, L. Falciola, P. Mussini, S, Righetto, D.

Roberto, R. Ugo, A. Valore, F. De Angelis, S. Fantacci, A. Sgamellotti, M. Ramon, M. Muccini, *Inorg. Chem.* **2007**, *46*, 8533.
[3] C. Dragonetti, S. Righetto, D. Roberto, R. Ugo, A. Valore, S. Fantacci, A. Sgamellotti, F. De Angelis, *Chem. Commun.* **2007**, 4116.
[4] C. Dragonetti, S. Righetto, D. Roberto, R. Ugo, A. Valore, F. Demartin, F. De Angelis, A. Sgamellotti, S. Fantacci, *Inorg. Chim. Acta* **2008**, *361*, 4070.
[5] C. Dragonetti, S. Righetto, D. Roberto, A. Valore, T. Benincori, F. Sannicolò, F. De Angelis, S. Fantacci, *J. Materials Science: Mater. Electron.* **2009**, *20*, 460.
[6] C. Dragonetti, S. Righetto, D. Roberto, A. Valore, *Phys. Status Solid C* **2009**, *6*, S50.
[7] a) B. F. Levine, C. G. Bethea, *Appl. Phys. Lett.* **1974**, *24*, 445; b) J. L. Oudar, *J. Chem. Phys.* **1977**, *67*, 446; c) K. D. Singer, A. F. Garito, *J. Chem. Phys.* **1981**, *75*, 3572; d) I. Ledoux, J. Zyss, *J. Chem. Phys.* **1982**, *76–77*, 203.
[8] a) J. Zyss, *Molecular Nonlinear Optics: Materials, Physics and Devices*, Academic Press, Boston, **1994**; b) *Optoelectronic Properties of Inorganic Compounds* (Eds.: D. M. Roundhill, J. P. Fackler Jr.), Plenum Press, New York, **1999**.
[9] For reviews on the application of PGSE NMR to the investigation of intermolecular interactions: B. Binotti, A. Macchioni, C. Zuccaccia, D. Zuccaccia, *Comments Inorg. Chem.* **2002**, *23*, 417. P. S. Pregosin, E. Martinez-Viviente, P. G. A. Kumar, *Dalton Trans.* **2003**, 4007. A. Bagno, F. Rastrelli, G. Saielli, *Prog. Nucl. Magn. Reson. Spectrosc.* **2005**, *47*, 41. T. Brand, E. J. Cabrita, S. Berger, *Prog. Nucl. Magn. Reson. Spectrosc.* **2005**, *46*, 159. Y. Cohen, L. Avram, L. Frish, *Angew. Chem.* **2005**, *117*, 524; *Angew. Chem. Int. Ed.* **2005**, *44*, 520. P. S. Pregosin, P. G. A. Kumar, I. Fernández, *Chem. Rev.* **2005**, *105*, 2977. P. S. Pregosin, *Prog. Nucl. Magn. Reson. Spectrosc.* **2006**, *49*, 261.
[10] a) N. K. Begum, E. Grunwald, *J. Am. Chem. Soc.* **1990**, *112*, 5104; b) E. Grunwald, K. C. Pan, *J. Phys. Chem.* **1976**, *80*, 2929.
[11] For details on the theoretical methods involved see Refs [34–40].
[12] A. Macchioni, *Chem. Rev.* **2005**, *105*, 2039.
[13] J. A. Mata, E. Peris, S. Uriel, R. Llusar, I. Asselberghs, A. Persoons, *Polyhedron* **2001**, *20*, 2083.
[14] M. P. Cifuentes, J. Driver, M. G. Humphrey, I. Asselberghs, A. Persoons, M. Samoc, B. Luther-Davies, *J. Organomet. Chem.* **2000**, *607*, 72.
[15] Nicolas Tancrez, Thèse de doctorat, Ecole Normale Supérieure de Cachan, France, **2005**.
[16] V. Alain, M. Blanchard-Desce, I. Ledoux-Rak, J. Zyss, *Chem. Commun.* **2000**, 353.
[17] L. Millán, M. Fuentealba, C. Manzur, D. Carrillo, N. Faux, B. Caro, F. Robin-Le Guen, S. Sinbandhit, I. Ledoux-Rak, J. R. Hamon, *Eur. J. Inorg. Chem.* **2006**, 1131.
[18] M. Fuentealba, L. Toupet, C. Manzur, D. Carrillo, I. Ledoux-Rak, J. R. Hamon, *J. Organomet. Chem.* **2007**, *692*, 1099.
[19] A. Macchioni, *Eur. J. Inorg. Chem.* **2003**, 195, and references therein.
[20] C. Zuccaccia, G. Bellachioma, G. Cardaci, A. Macchioni, B. Binotti, C. Carfagna, *Helv. Chim. Acta* **2006**, *89*, 1524. M. S. Lowry, W. R. Hudson, R. A. Pascal, S. Bernhard, *J. Am. Chem. Soc.* **2004**, *126*, 14129.
[21] D. Zuccaccia, A. Macchioni, *Organometallics* **2005**, *24*, 3476.
[22] A. Macchioni, G. Ciancaleoni, C. Zuccaccia, D. Zuccaccia, *Chem. Soc. Rev.* **2008**, *37*, 479–489.
[23] G. Ciancaleoni, C. Zuccaccia, D. Zuccaccia, A. Macchioni, *Organometallics* **2007**, *26*, 3624.
[24] S. Pettirossi, G. Bellachioma, G. Ciancaleoni, C. Zuccaccia, D. Zuccaccia, A. Macchioni, *Chem. Eur. J.* **2009**, *15*, 5337.
[25] M. Wien, *Phys. Z. Sowjetunion* **1931**, *32*, 545.
[26] L. Onsager, *J. Chem. Phys.* **1934**, *2*, 599.
[27] According to reference [32] it was estimated a 40% increase of the ion-pair dissociation constant.
[28] A. Valore, PhD Thesis, Università degli Studi di Milano (Italy), **2009**.
[29] J. Jeener, B. H. Meier, P. Bachmann, R. R. Ernst, *J. Chem. Phys.* **1979**, *71*, 4546–4563.
[30] R. Wagner, R. Berger, *J. Magn. Reson. Ser. A* **1996**, *123*, 119–121.
[31] B. Lix, F. D. Sonnichsen, B. D. Sykes, *J. Magn. Reson. Ser. A* **1996**, *121*, 83–87.
[32] M. Valentini, H. Rüegger, P. S. Pregosin, *Helv. Chim. Acta* **2001**, *84*, 2833.
[33] a) H. J. W. Tyrrell, K. R. Harris, *Diffusion in Liquids*, Butterworth, London, **1984**; b) R. Mills, *J. Phys. Chem.* **1973**, *77*, 685–688.
[34] A. D. Becke, *Phys. Rev. A* **1988**, *38*, 3098; J. P. Perdew, *Phys. Rev. B* **1986**, *33*, 8822.
[35] G. te Velde, F. M. Bickelhaupt, E. J. Baerends, C. Fonseca-Guerra, S. J. A. van Gisbergen, J. G. Snijders, T. Ziegler, *J. Comput. Chem.* **2001**, *22*, 931.
[36] Gaussian 03, Revision B.05, M. J. Frisch, G. W. Trucks, H. B. Schlegel, G. E. Scuseria, M. A. Robb, J. R. Cheeseman, J. A. Montgomery, Jr., T. Vreven, K. N. Kudin, J. C. Burant, J. M. Millam, S. S. Iyengar, J. Tomasi, V. Barone, B. Mennucci, M. Cossi, G. Scalmani, N. Rega, G. A. Petersson, H. Nakatsuji, M. Hada, M. Ehara, K. Toyota, R. Fukuda, J. Hasegawa, M. Ishida, T. Nakajima, Y. Honda, O. Kitao, H. Nakai, M. Klene, X. Li, J. E. Knox, H. P. Hratchian, J. B. Cross, C. Adamo, J. Jaramillo, R. Gomperts, R. E. Stratmann, O. Yazyev, A. J. Austin, R. Cammi, C. Pomelli, J. W. Ochterski, P. Y. Ayala, K. Morokuma, G. A. Voth, P. Salvador, J. J. Dannenberg, V. G. Zakrzewski, S. Dapprich, A. D. Daniels, M. C. Strain, O. Farkas, D. K. Malick, A. D. Rabuck, K. Raghavachari, J. B. Foresman, J. V. Ortiz, Q. Cui, A. G. Baboul, S. Clifford, J. Cioslowski, B. B. Stefanov, G. Liu, A. Liashenko, P. Piskorz, I. Komaromi, R. L. Martin, D. J. Fox, T. Keith, M. A. Al-Laham, C. Y. Peng, A. Nanayakkara, M. Challacombe, P. M. W. Gill, B. Johnson, W. Chen, M. W. Wong, C. Gonzalez, J. A. Pople, Gaussian, Inc., Pittsburgh PA, **2003**.
[37] A. D. Becke, *J. Chem. Phys.* **1993**, *98*, 5648.
[38] P. J. Hay, W. R. Wadt, *J. Chem. Phys.* **1985**, *82*, 270.
[39] S. Mierts, S. Scrocco, T. Tomasi, *Chem. Phys.* **1981**, *55*, 117.
[40] a) A. Willetts, J. E. Rice, D. M. Burland, D. P. Shelton, *J. Chem. Phys.* **1992**, *97*, 7590; b) D. R. Kanis, M. A. Ratner, T. J. Marks, *Chem. Rev.* **1994**, *94*, 195.

Received: October 9, 2009
Revised: January 5, 2010
Published online: March 18, 2010

